JOURNAL OF MATERIALS SCIENCE 28 (1993) 2105–2111

Interdiffusion-induced devitrification of porcelain enamel on steel

H. H. LIU, P. SHEN
Institute of Materials Science and Engineering, National Sun Yat-Sen University, Kaohsiung, Taiwan

Y. SHUEH, F. S. YANG
New Materials R & D Department, China Steel Corporation, Kaohsiung, Taiwan

Devitrification which occurred in the ground coat (fired at 830 °C for 0–30 min) due to interdiffusion near the steel–enamel interface was characterized by electron microscopy (SEM and TEM) coupled with energy-dispersive X-ray analysis. Spinel oxide, Fe_3O_4, which was alloyed with Ni if nickel-dip pre-treatment was adopted and was compatible with α-Fe, crystallized in the ground coat near the glass–metal interface. Independent of nickel-dip pre-treatment the spinel crystals were extensively developed at the edges of the specimen slab, but were fewer and smaller in the centre of the flat faces. The quantity and size of crystals increased with the firing time. Within the titania-opacified cover coat (fired subsequently at 800 °C for 3 min) equiaxed TiO_2 crystals (anatase with a minor amount of rutile) were distributed uniformly. The TiO_2 crystals grew inwards to some extent into the ground coat and became needle-like with their long axes aligned diagonally to the interface. The devitrification of enamel was affected significantly by diffusion across the interfaces which resulted in a saturation with oxide components.

1. Introduction

Refractory oxides such as spinel phases have been found at the metal–ceramic interface in a number of systems. Examples include precipitation in an early magmatic stage, oxidized out of the slagged matte [1], and in cermets such as NiAl–$ZrO_2(Y_2O_3)$ and Ni_2AlTi–$ZrO_2(Y_2O_3)$ [2]. The occurrence of silicate phases in glass–ceramics on various metal substrates has also been recognized [3], e.g. lithium disilicate and quartz have been found in the Li_2O–ZnO–SiO_2 coating to mild steel and the quality of the bond to the metal depends on the compatibility of the lithium iron silicate phase with the metal substrate [3, 4].

The occurrence of a crystalline phase has also been recognized in porcelain enamel containing oversaturated Fe_3O_4 in the batch [5], though the crystal structure was not clarified. The ground-coat batch of enamelled steel generally does not fall in the composition range for devitrification; however, interdiffusion with steel and consequent saturation of cations in glass may cause local devitrification of the glass. The possibility of interdiffusion and its resultant devitrification of enamel, which may affect the quality of the bond to the metal, was not reported. In the system of enamelled steel, attention has been paid mainly to the factors which are important for promoting adherence of enamel to steel, including the catalytic activity of nickel or cobalt which enhances the roughness at the interface [5–14]. Recent transmission electron microscopy (TEM) results indicated that the adherence is controlled partly by epitaxial oxide particles of spinel (R_3O_4, where R represents cations of iron and minor nickel) which are intimately mixed with α-iron [15]. However, the microstructure of the porcelain enamel due to devitrification was not studied by TEM and the effect, if any, of nickel-dip pre-treatment on devitrification was not known.

A titania-opacified cover coat is commonly overlain on the ground coat of enamelled steel. Metallographic and X-ray diffraction studies have indicated that the cover coat contains anatase and/or rutile in a glass matrix [16]. However, the microstructure of TiO_2 crystals in the cover coat and the effect of interdiffusion between cover coat and ground coat on the microstructure of the TiO_2 crystals were not known.

Reported here are the results of our electron microscopy observations of the devitrification products of porcelain enamels (ground coat or two-coat) on steel slabs which were either pickled or nickel-pickled. The identity and morphology of crystals in the ground coat, titania-opacified cover coat, and at interfaces were studied by TEM. Attention has also been paid to the devitrification behaviour at the edges of the slab sample in contrast to that at the flat faces.

2. Experimental procedure

Detailed procedures to prepare the ground coat on Ti-stabilized low-carbon steel with pretreatments of degreasing, pickling, nickel dip and neutralization

0022–2461

were given elsewhere [15]. The enamel batch of ground coat contains 30% water, frit powders from Ferro Co. (24% 2220, 18% 2212, 18% 2216) and powders of 6% quartz, 4% kaolinite, 0.1% borax and 0.09% $NaNO_3$ (wt %) which were mixed by ball (Al_2O_3) milling for 2 h to prepare the enamel slurry [15]. The iron content in the frit batch of the ground coat is far less than that required for saturation, therefore the effect of interdiffusion can be evaluated. Suspension specimen slabs (Fig. 1) which had been immersed in the enamel slurry and dried were fired in an open-air furnace. Owing to the slight decrease of temperatures when specimens were inserted into the furnace, the firing time was not set until the temperature rose back to the preset value [15]. After firing, specimens were withdrawn from the furnace and air-cooled [15].

Commercial frits (Ferro Co., 7266) which contain mainly oxide components of Si, Ti, Na, Al, K, Zn and Zr in decreasing weight percentage other constituents such as Ca, Fe and Co are about tens of p.p.m. were ball (Al_2O_3) milled and sieved through 120 mesh before making batches of enamel. The slurry of the cover-coat batch contained ca. 30% water and powders of 67% 7266, 3% kaolinite and 0.2% $NaAlO_2$ (wt %). Following previous practice [15], five digit numbers followed by the letters N and/or P were designated to the ground-coated slabs, where the first three digits (830) represent temperature 830 °C, the last two digits firing time, and N and P represent nickel and pickle treatment, respectively. The 83003NP specimen was chosen for the subsequent cover coating (800 °C for 3 min) by the same immersion and firing procedures as for ground coating.

Optical microscopy under reflected light and scanning electron microscopy (SEM, JSM35CF, 25 kV) coupled with energy-dispersive X-ray (EDX) analysis were used for microstructure and qualitative composition characterization of the polished or Nital-etched surface sliced perpendicular to the coating interface. Thin sections of cover-coated specimen 83003NP excluding slab edges were cut perpendicular to the interface and ground (Gatan 623) to about 20 μm in thickness, then ion-milled to electron transparency and subsequently studied by TEM (Jeol 200CX) coupled with EDX analysis at 200 kV. X-ray (CuK_α) diffraction was also used for identification of crystalline phases.

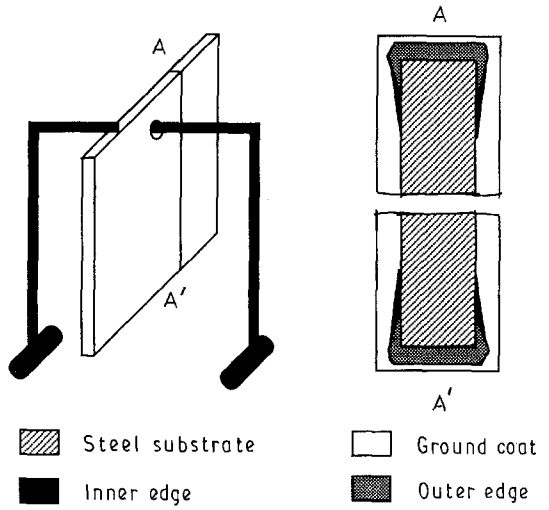

Figure 1 Configuration of the suspension slab specimen and pottery rack during firing. Cross-section AA' shows the extensive devitrification regions near the steel substrate which has been ground-coated.

3. Results

Unless specified, the observations described in the following for pickled specimens apply also to the nickel-pickled specimens, and vice versa.

3.1. Optical observations

The surface of the two-coat enamelled steel appears white and free of fish-scale to the naked eye. Optical microscopy observations (under reflected light) of cross-sections of the ground-coat slab showed that near the substrate–coating interface, extensively devitrified outer edges of about 0.5 mm in width, less devitrified inner edges, and least devitrified centre of faces were formed (Fig. 1), and this is true regardless of the firing time for ground coating and the subsequent overlay of the cover coating. Spinel crystals were extensively developed at the devitrified outer edge of the slab specimen which had been fired with negligible time at 830 °C (Fig. 2a), and their quantity and size increased with an increase of firing time (Fig. 2b). For cross-sections of the least devitrified centre of faces,

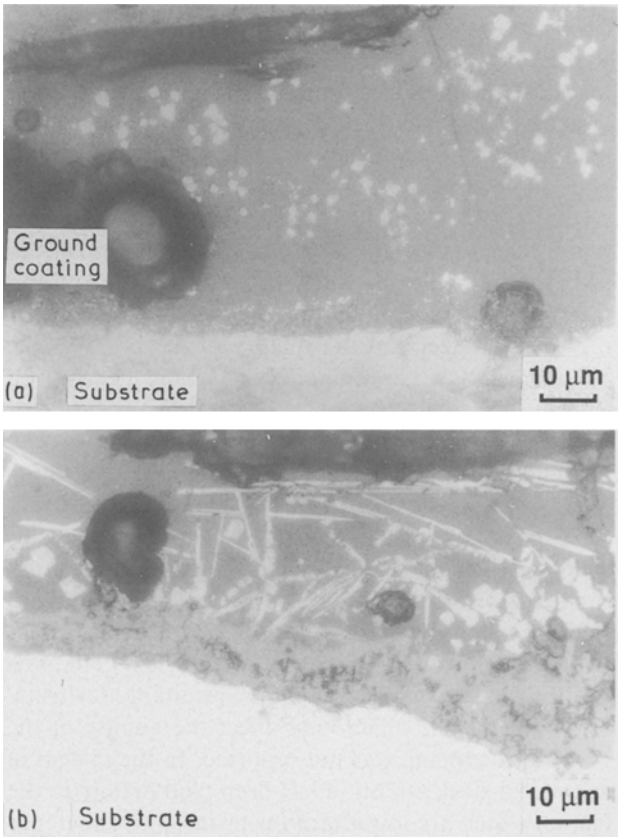

Figure 2 Cross-section micrograph (optical reflected light) of ground coat and substrate, sectioned from outer edge of the specimen slab. Note spinel oxide crystals in devitrified enamel near the metal substrate (bright): (a) 83000P, (b) 83030P, both Nital-etched.

optical microscopy failed to detect the occurrence of spinel oxides or other crystalline phases in enamel near the substrate, including samples fired further at 800 °C for cover coating (Fig. 3). The cover coat reflects more light than the ground coat, both being about 100 μm in thickness, and includes bubbles tens of micrometres in diameter.

3.2. SEM–EDX analysis

SEM observation cannot reveal individual TiO_2 crystals in the cover coating, but devitrification of ground coat near the steel substrate can be readily analysed due to the significant composition difference between the devitrification products and the enamel matrix. Fig. 4 shows back-scattered electron images (BSE images) of the cross-section of the extensively devitrified outer edge of the ground coat, showing crystals in devitrified enamel near the metal substrate. It is noteworthy that firing isochronally (30 min) at 830 °C caused the formation of crystal particles in both the nickel-pickled specimen (Fig. 4a) and the pickled specimen (Fig. 4b), but crystals with well-developed facet planes also occurred in the outer zone in the pickled specimen (Fig. 4b). EDX analysis (Fig. 4c) and parallel X-ray diffraction indicated that the crystals are Fe-bearing spinel oxide which may contain Ni (i.e. Fe_3O_4–$NiFe_2O_4$ solid solution) if nickel-dip pre-treatment was adopted. Besides spinel oxide, metal particles were also found in the less devitrified inner edge (Fig. 1) of 83030NP specimen (Fig. 5a). According to SEM–EDX analysis, these metal particles are rich in Fe and Ni (from nickel-dip pre-treatment) and appear bright (similar to the metal substrate in the BSE image), but the neighbouring spinel oxides appear grey, having less or even negligible Ni content (Fig. 5b). According to the iron–nickel–oxygen phase diagram at 1000 °C [17], there is an extensive coexistence phase field of Fe–Ni alloy and Fe_3O_4–$NiFe_2O_4$ spinel solid solution. This explains the coexistence of metal particles and spinel oxide in the ground coat, and the occurrence of spinel particles intimately mixed with the iron matrix [15]. On the basis of the above

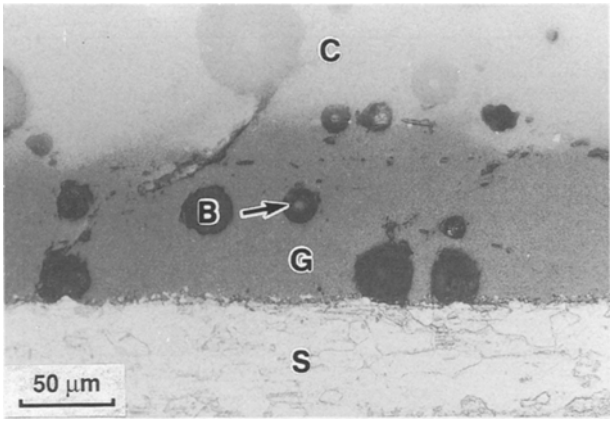

Figure 3 Cross-section micrograph (optical reflected light) of two-coat (ground coat: G, cover coat: C) enamelled steel cut excluding the slab edges (83003NP, then cover-coated at 800 °C for 3 min). Note bubbles (B) in both coatings (Nital-etched).

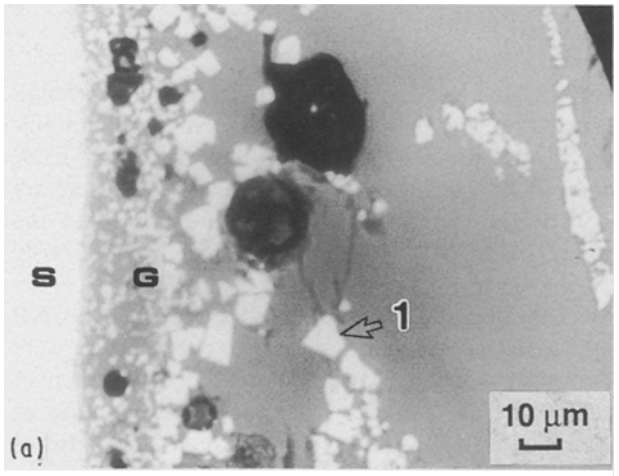

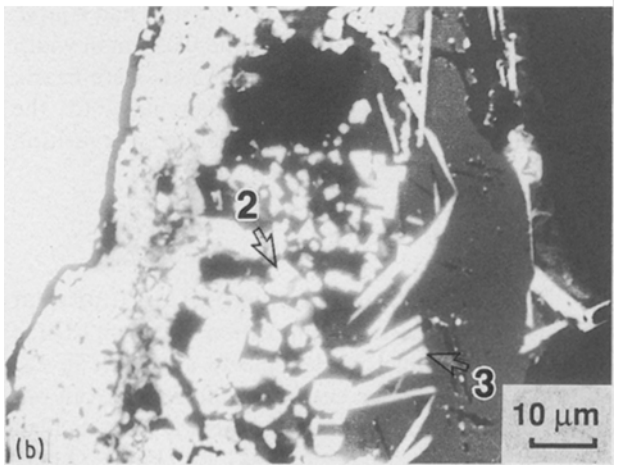

Figure 4 Representative SEM (BSE image) of ground-coated (G) sample cross-sectioned from outer edge of the specimen slab, showing spinel crystals (bright) in devitrified enamel (dark) near the metal substrate (S): (a) 83030NP, (b) 83030P, (c) EDX analyses on points 1, 2 and 3 arrowed in (a) and (b).

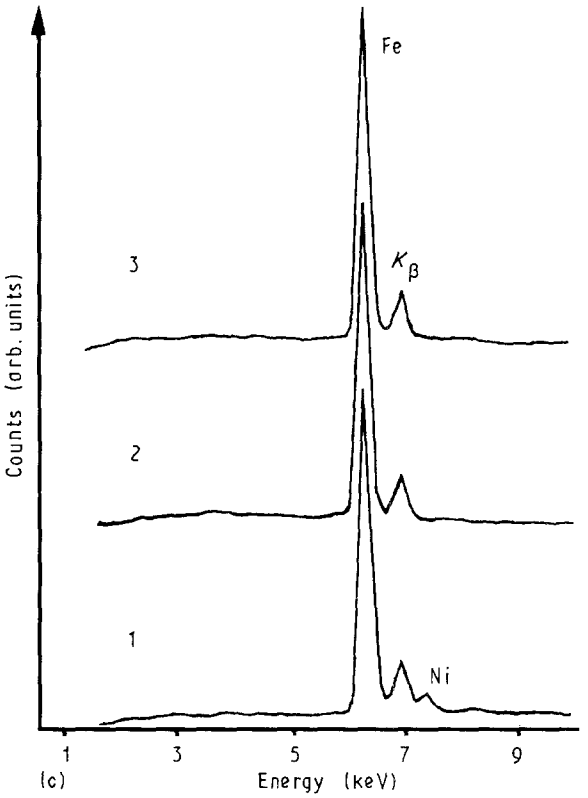

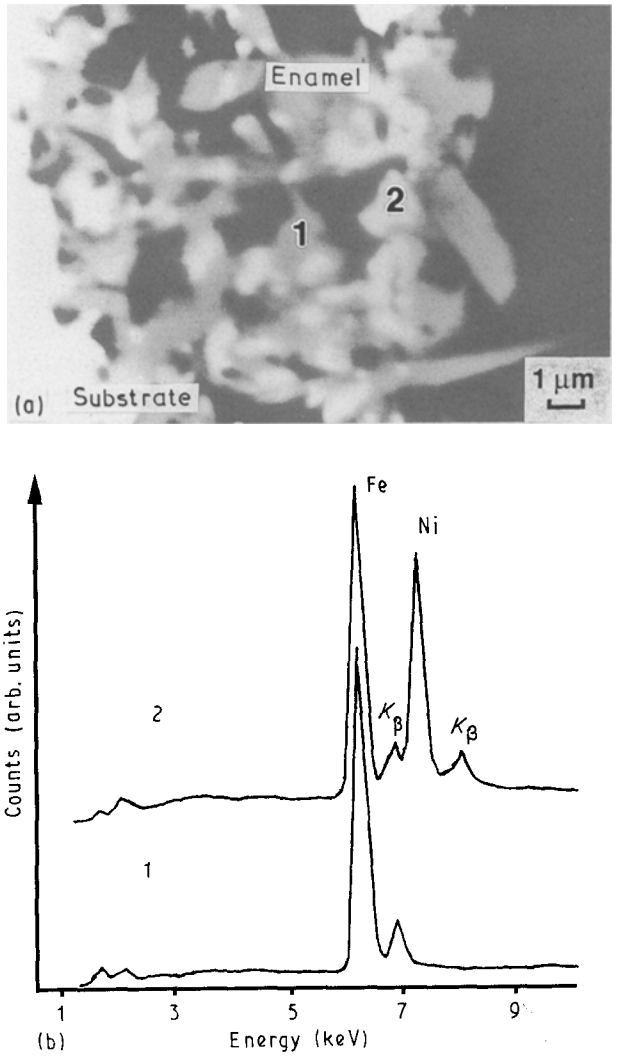

Figure 5 (a) Magnified BSE image of cross-section from inner edge of 83030NP specimen showing metal island (bright) besides spinel oxide (grey) in the matrix of enamel (dark) adjacent to the metal substrate (bright); (b) EDX analyses at points 1 and 2 indicated.

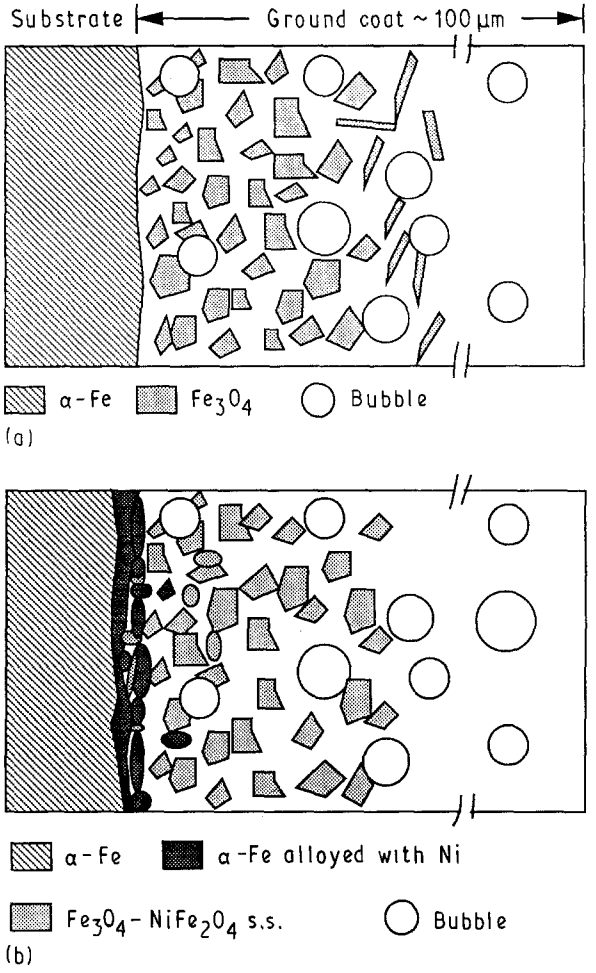

Figure 6 Schematic drawing of cross-sections from slab edges showing extensive formation of spinel oxide in enamel for (a) pickled and (b) nickel-pickled specimen.

results, the cross-sections of the devitrified enamel at the slab edges are depicted in Fig. 6a and b for pickled and nickel-pickled specimens, respectively. It is noteworthy that the phase assemblages are the same for both specimens, but the nickel-pickled specimen has a rougher interface and has an Ni-alloyed Fe layer and islands due to the catalytic effect of nickel at the interface [15].

3.3. TEM observations

STEM–EDX analysis of the TEM foil which was sectioned excluding the extensively devitrified edges of cover-coated specimen 83003NP (Fig. 1) indicated also the occurrence of Fe- and Ni-bearing particles near the steel–enamel interface (Fig. 7). Electron diffraction indicated that these particles are also spinel crystals, but are much smaller (submicrometre in size) than those at the edges of the specimen slabs. STEM–EDX analysis of enamel always showed high Fe content in the vicinity of the steel–enamel interface. Microcline (K-feldspar) which has modulated contrast (Fig. 8a) and contains Al, K, Si and Fe was occasionally identified on selected-area diffraction (SAD) patterns and by STEM–EDX analysis (Fig. 8b). Small crystals ranging from 0.1 to 1 μm in size and containing Si and other cations according to STEM–EDX analysis also occurred in the ground coat. These are silicates, more likely to be less refractory than the spinel oxide because the former commonly vitrify during exposure to the electron beam.

TEM analysis of cover-coated specimen 83003NP indicated that TiO_2 crystals about 0.1 μm in size were uniformly distributed in the glass matrix of the cover coat (Fig. 9a). These crystals are mainly anatase as identified by X-ray diffraction, although SAD patterns indicating rutile also occurred (Fig. 9b). At the ground–cover coat interface, TiO_2 crystals had a large aspect ratio, e.g. 0.5 μm in length and 0.05 μm in width (Fig. 9c). These needle-like TiO_2 crystals were nearly aligned with their long axes diagonally to the ground–cover coat interface, and defined a transition zone.

4. Discussion

4.1. Devitrification mechanism of ground coat

Analogous to the other composition systems [18] the coexistence of spinel oxide, silicate and melt in the ground coat suggests a eutectic or more likely an off-eutectic melting for the enamel batch. Due to its high melting point (e.g. $T_m \sim 1600\,°C$ for Fe_3O_4 [19]),

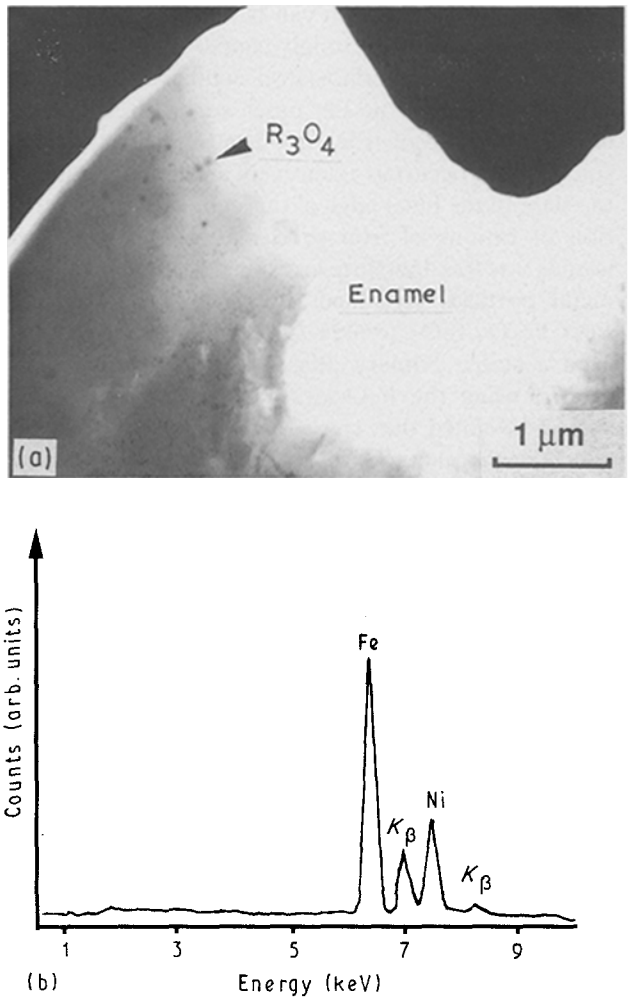

Figure 7 TEM of spinel oxide particles in ground coat: (a) bright-field image, (b) STEM–EDX analysis of spinel; specimen 83003NP, cross-section foil prepared excluding the extensively devitrified slab edges.

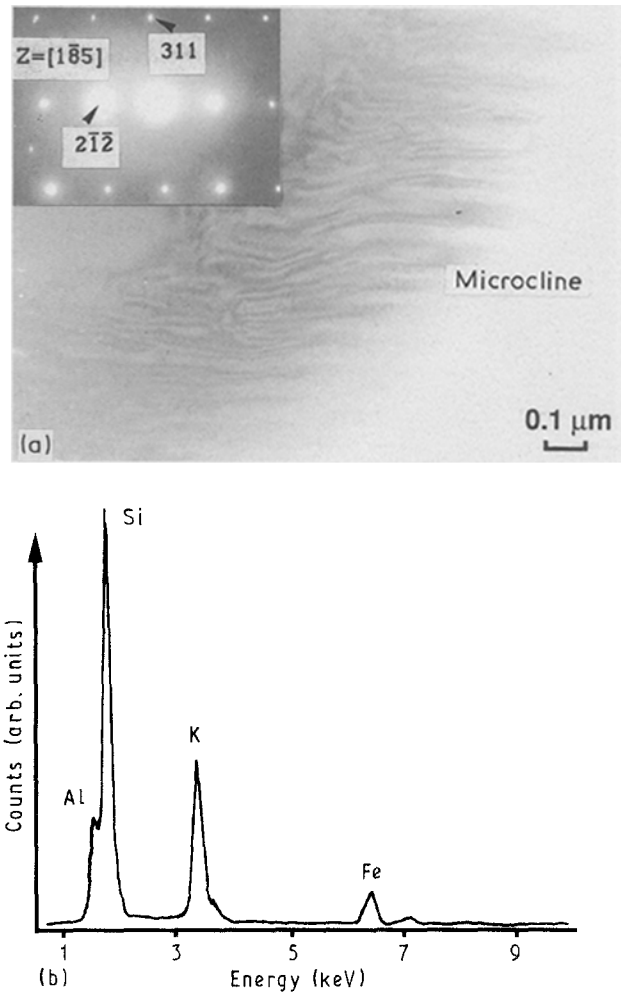

Figure 8 TEM of modulated microcline in ground coat: (a) BF image, SAD pattern is inset; (b) STEM–EDX analysis of microcline, same specimen as Fig. 7.

spinel oxide may crystallize in the incipient stage from a cooling melt. However, the occurrence of crystalline phases in enamel near the steel substrate and at the slab edges indicates that the devitrification kinetics of the ground coat was not affected only by temperature.

Under constant firing conditions, devitrification kinetics of the ground coat could possibly be affected by the tramp impurities in the enamel batch which trigger heterogeneous nucleation, and surface nucleation at interfaces or at bubbles. Other factors such as (i) undercooling, (ii) saturation of cations derived from the steel substrate, and (iii) composition dependence of viscosity of the melt or glass which may be relevant to the formation of spinel oxide crystals in ground coating are discussed successively in the following.

4.1.1. Undercooling

According to Kirkpatrick's [20] summary on the undercooling dependence of the crystallization behaviour of rocks of lunar composition, vicinal interfaces develop differently for (a) growth controlled by screw dislocations emergent at the centre of the face at low undercoolings, and (b) surface nucleation-controlled growth at relatively large undercoolings. Under condition (b), the rate of generation of steps increases rapidly with increasing undercooling, and more layers will be generated at corners or edges, which are at larger undercoolings than the face centres. However, the occurrence of larger spinel crystals at the edges of the slab and smaller crystals at the centre of the face cannot necessarily be attributed to larger undercooling at the edge than at the centre of the face because devitrification at slab edges was enhanced significantly with firing time, and no sidearms or dendrites which are characteristic of undercooling were found.

4.1.2. Saturation of iron oxide in enamel

STEM–EDX analysis of enamel showed high Fe content in the vicinity of the steel–enamel interface, indicating that the formation of spinel in the ground coat was most likely to be due to the saturation of iron derived from the steel substrate. Electron microprobe analysis of the diffusion profiles of FeO in enamel fired at 805 °C for 36 to 1200 s [21] also indicated a high and constant FeO content (0.283 g cm^{-2}) at the interface and a diffusion coefficient of 1.3×10^{-8} cm^2 s^{-1} calculated from diffusion profiles. The presence of excess iron oxide at all times (36 to 1200 s) and the constant FeO source indicated saturation of the

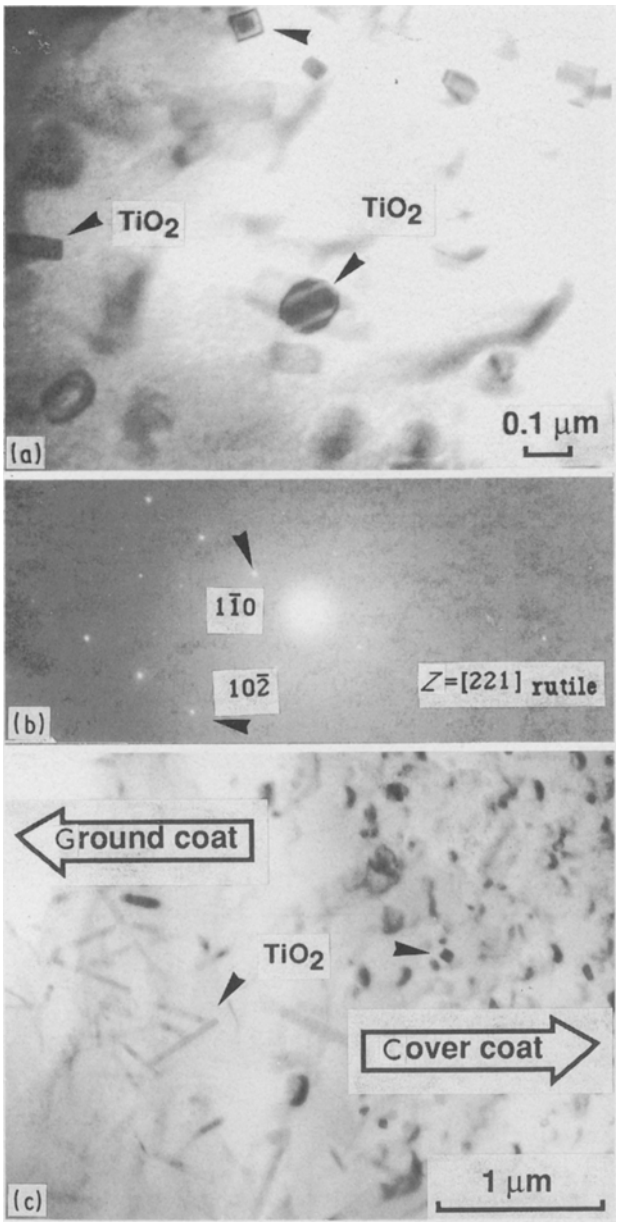

Figure 9 TEM of TiO_2-bearing coating: (a) TiO_2 crystals in cover coat (BF image), (b) SAD pattern of a rutile particle, (c) BF image showing needle-like TiO_2 crystals distributed between ground coat and cover coat (same specimen as Fig. 7).

enamel with iron oxide at the interface [21]. TEM observation of spinel particles either in the substrate [15] or in the enamel as shown in the present study is also consistent with the idea that iron oxide saturation led to devitrification of the enamel. Since the iron content in the frit batch of the ground coat [15] is far less than that required for saturation, the ultimate cause of spinel crystals is therefore the saturation of the enamel with iron oxide due to diffusion across the enamel–steel interface, rather than being derived from the ground coat batch. It is noteworthy that compared to iron oxides of other stoichiometry the spinel oxide is more compatible with α-Fe particles or the substrate because the thermal mismatch between spinel and α-Fe is small [15], and they are in equilibrium over large temperature and composition ranges [17]. It follows that the extensive crystallization of spinel oxide in enamel near the metal–enamel interface did not affect the quality of the bond to the metal.

Ferric and ferrous iron can be dissolved in silicate melts and the ratio is strongly temperature-dependent [22]. Because the interface (steel–enamel) area per unit volume is greatest at the outer edge, saturation of ferrous and/or ferric irons, and hence the formation of spinel oxide, occurred extensively at the outer edge of the slab. In the inner edge of the slab (Fig. 5a), saturation of cations of iron or oxidation of nickel-rich islands was less, therefore less spinel oxide formed and metal particles remained. In certain areas of the $FeO–Fe_2O_3–SiO_2$ ternary system [19], iron was indeed a stable primary phase, and was observed in enamel using the FeO-saturated base glass [5]. It should be noted that spinel phase may have formed after the metal particles and it appeared equiaxed especially for the nickel-pickled specimen (Fig. 4a), but it may also have crystallized from the melt and have well-developed facet planes as for the pickled specimen (Fig. 4b).

4.1.3. Viscosity

Because of the composition dependence of viscosity [23], the dissolution of cations derived from steel (Fe^{2+}/Fe^{3+}) and nickel-dip (Ni^{2+} or Ni^{3+}), and other components derived from the enamel batch could also affect crystallization behaviour. Viscosity may affect the segregation of the crystals in a melt according to Stokes's law; however, the possibility of segregation of spinel oxides due to gravity was excluded because larger spinel crystals were found at all edges of the suspension slabs (Fig. 1).

4.2. Crystallization of TiO_2

Formation of TiO_2 crystals in the cover coat must have occurred during firing because the cover coat frit is amorphous according to X-ray diffraction. There are three polymorphs of TiO_2 (anatase, brookite, rutile) known to occur under ambient conditions in nature. Therefore, it is not certain which one is the thermodynamically stable modification, although brookite is often considered to be of secondary origin [24]. According to Eppler and McClaren [25, 26], crystallization and phase transformation in TiO_2-opacified porcelain enamels include: (1) crystallization of anatase, (2) crystallization of rutile, and (3) transformation of anatase to rutile. TiO_2 crystals in the present sample remained mainly as anatase; this suggests, according to Eppler and McLaren [25, 26], that the transformation of anatase to rutile was limited at 800 °C. Undercooling played a negligible role in the shape and growth of TiO_2 crystals, because no side arms or dendrites were observed.

In the transition zone between ground coat and cover coat, TiO_2 crystals are elongated and aligned with their long axes diagonally to the ground coat–cover coat interface (Fig. 9). An elongated TiO_2 crystal with its long axis parallel to the *c* axis commonly occurs because both anatase and rutile have edge-sharing polyhedra along the *c* axis [27]. In anatase the shared edges at top and bottom of the octahedra are at right-angles to each other, while in rutile

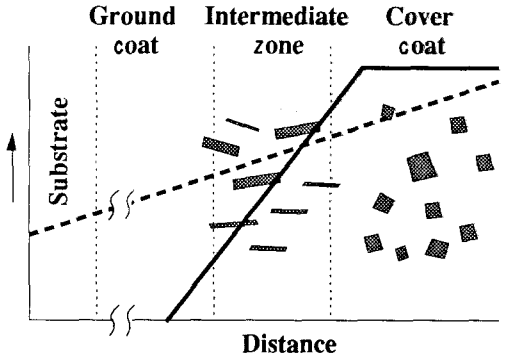

Figure 10 Schematic drawing showing the possible (—) concentration gradient of TiO_2 and (---) temperature variation across the enamel during firing; the resultant distribution and morphology of TiO_2 crystals (shown shaded) are also depicted.

two opposite parallel edges are shared [27]. A possible temperature gradient during firing and a TiO_2 concentration gradient (based on SEM–EDX analysis) across the coatings are depicted schematically in Fig. 10. The occurrence of roughly aligned needle-like TiO_2 crystals in the transition zone but not in the cover coat was probably not caused by temperature distribution of the slab specimen during firing or cooling. Instead, it is suggested that during firing a TiO_2 concentration gradient developed in the transition zone due to interdiffusion across the ground coat–cover coat interface region, both being boron- and sodium-bearing silicate glasses. The directional supply of Ti^{4+} from the cover coat then resulted in the saturation of the nearby ground coat with titanium oxide and the crystallization of TiO_2 crystals aligned diagonally to the ground coat–cover coat interface. Nuclei of TiO_2 crystals could also migrate inwards and facilitated further crystallization.

5. Conclusions

Devitrification of enamel occurred as soon as the set temperature for ground coating on steel was reached and the phase assemblages of the coating were not affected by nickel-dip pre-treatment. It is suggested that devitrification was affected by diffusion across the interfaces and the consequent saturation of oxide components in the enamels. The main findings from electron microscopy are as follows.

1. Fe-bearing spinel oxide (which may contain Ni if nickel-dip pre-treatment was adopted) formed in the ground coat near the enamel–metal interface.
2. Spinel oxide was extensively developed at the slab edges, but was much smaller at the centres of the flat faces of the slab specimen, and its quantity and size increased with increase of firing time.
3. TiO_2 crystals (anatase with a minor amount of rutile) grew inwards to some extent into the ground coat and became needle-like, aligned with their long axes diagonally to the interface.
4. The extensive crystallization of spinel oxide in enamel near the enamel–metal interface did not affect the quality of the bond to the metal.

Acknowledgement

We thank Mr W. Deng for ion-milling the TEM sample.

References

1. J. D. GILCHRIST, "Extraction Metallurgy" (Pergamon, Oxford, 1980) p. 229.
2. P. SHEN and S. L. HWANG, *Mater. Sci. Eng.* **100** (1988) 177.
3. G. PARTRIDGE, C. A. ELYARD and M. I. BUDD, in "Glasses and Glass Ceramics", edited by M. H. Lewis (Chapman and Hall, London 1989) p. 226 and literature cited therein.
4. A. J. STURGEON, D. HOLLAND, G. PARTRIDGE and C. A. ELYARD, *Glass Technol.* **27** (1986) 102.
5. B. W. KING, H. P. TRIPP and W. H. DUCKWORTH, *J. Amer. Ceram. Soc.* **42** (1959) 504.
6. J. H. HEALY and A. I. ANDREWS, *ibid.* **34** (1951) 214.
7. *Idem, ibid.* **34** (1951) 207.
8. W. N. HARRISON, J. C. RICHMOND, J. W. PITTS and S. G. BENNER, *ibid.* **35** (1952) 113.
9. M. P. BOROM and J. A. PASK, *ibid.* **49** (1966) 1.
10. G. S. DOUGLAS and J. M. ZANDER, *ibid.* **34** (1951) 52.
11. U. F. UHER, *Proc. PEI Forum* **32** (1970) 156.
12. M. A. SALAMAH and D. WHITE, *J. Amer. Ceram. Soc.* **64** (1981) 224.
13. J. D. SULLIVAN, *Ceram. Eng. Sci. Proc.* **2** (1981) 143.
14. J. A. PASK, *Amer. Ceram. Soc. Bull.* **66** (1987) 1587.
15. H. H. LIU, Y. SHUEH, F. S. YANG and P. SHEN, *Mater. Sci. Eng.* (A) **149** (1992) 217.
16. R. F. PATRICK, *J. Amer. Ceram. Soc.* **34** (1951) 96.
17. A. D. DALVI and W. W. SMELTZER, *J. Electrochem. Soc.* **117** (1970) 1431.
18. R. M. EL-SHAHAT and J. WHITE, *Trans. Br. Ceram. Soc.* **65** (1966) 497.
19. E. M. LEVIN, C. R. ROBBINS and H. F. McMURDIE, "Phase Diagram for Ceramists" (American Ceramic Society, Columbus, Ohio, 1964) p. 38.
20. R. J. KIRKPATRICK, in "Kinetics of Geochemical Processes", edited by A. C. Lasaga and R. J. Kirkpatrick (Mineralogical Society of America, Washington D.C., 1981) p. 367 and literature cited therein.
21. D. RITCHIE, H. A. SCHAEFFER and D. WHITE, *J. Mater. Sci.* **18** (1983) 599.
22. R. A. LANGE and I. S. E. CARMICHAEL, *Geochem. Cosmochem. Acta* **53** (1989) 2195 and literature cited therein.
23. B. O. MYSEN, "Structure and Properties of Silicate Melts" (Elsevier, New York, 1988) p. 147 and literature cited therein.
24. L. G. LIU and W. A. BASSETT, "Elements, Oxides and Silicates: High-Pressure Phases with Implications for the Earth's Interior" (Oxford University Press, New York, 1986) p. 115.
25. R. A. EPPLER and W. A. McLAREN Jr., *J. Amer. Ceram. Soc.* **50** (1967) 152.
26. R. A. EPPLER *ibid.* **52** (1969) 94.
27. W. A. DEER, R. A. HOWIE and J. ZUSSMAN, "An Introduction to the Rock-Forming Minerals", (Longmans Green, London, 1966) p. 415.

Received 14 October 1991
and accepted 14 August 1992